

ANN and FA Based Design of Hybrid Fractal Antenna for ISM Band Applications

Manpreet Kaur* and Jagtar S. Sivia

Abstract—In this paper, a compact Giuseppe Peano, Cantor Set, and Sierpinski Carpet fractals based hybrid fractal antenna (GCSA) is designed and developed for Industrial, Scientific and Medical (ISM) band applications. The proposed GCSA is a hybrid fractal design which is created by fusing Giuseppe Peano, Cantor set, and Sierpinski carpet fractals together. The optimization of the microstrip line feed position is performed by using a Firefly Algorithm (FA). The substrate material employed for proposed GCSA is a low-priced, easily available FR4 epoxy of thickness 1.6 mm. By varying the geometrical dimensions of the radiating patch, a data set of 58 GCSAs is randomly generated for the realization of Artificial Neural Network (ANN) and FA approaches. The designed structure is fabricated, and then measured results are evaluated. The proposed GCSA is capable of resonating at 2.4450 GHz with $S(1,1) < -10$ dB. The measured bandwidth of the operating ISM band is 101 MHz. The quantitative performance of three different ANN types reveals that Feed Forward Back Propagation ANN (FFBPN) shows minimum error in comparison to other two ANN types. The simulated, experimental, and optimized results show a good match that specifies the preciseness of the measurement.

1. INTRODUCTION

Biomedical engineering is a rapidly growing field that focuses on the development related to human health care at distinct levels [1]. This branch deals with the continuous evaluation of several important physiological parameters such as sugar level and pulse rate, blood pressure [2, 3]. Antennas play a crucial role in transmitting biological signals to remote health care centers so that patients can receive proper treatment at the right time [4]. Fractal and hybrid fractal antennas have several applications in various engineering disciplines [5]. Fractals are defined as nonuniform or asymmetrical fragments that characterize a complicated set of structures that repeat themselves at different scales [6, 7]. The two fundamental properties of fractals help to generate distinct magnificent fractal designs that produce more diversified current distribution and hence provide superior radiation characteristics [8, 9]. The emerging hybrid fractal technology employs the integration of distinct fractal shapes for the construction of novel antennas that exhibit unique characteristics [10]. The design of a fractal or hybrid fractal antenna for particular operating frequencies is a complicated task because the standard mathematical procedures and exact expressions don't exist [11]. Therefore, the implementation of miniaturized fractal and hybrid fractal antennas is a prime field of research these days. Several hybrid fractal antenna designs based on different fractal shapes have been reported in [12–16].

Minkowski curves, Hilbert curves, Sierpinski carpet, Giuseppe Peano and Cantor set fractals have fascinated multiple researchers to create miniaturized antennas with good functionalities [17–20]. Salim and Pourziad [21] have explained a compact structure of the reconfigurable spiral-shaped antenna that operates for important biomedical bands. A simple ultra-wideband (UWB) fractal antenna

Received 9 November 2019, Accepted 15 December 2019, Scheduled 31 December 2019

* Corresponding author: Manpreet Kaur (sketty@rediffmail.com).

The authors are with the Yadavindra College of Engineering, Punjabi University Guru Kashi Campus, Talwandi Sabo, Bathinda, Punjab, India.

that was generated by the application of Giuseppe Peano and Sierpinski carpet fractals is described in [22]. Choukiker and Behera [23] have investigated the operation of a wideband fractal antenna which was composed of two distinct types of fractals. Oraizi and Hedayati [24] have demonstrated the performance of a multiband antenna structure which was realized by the fusion of different fractals designs. A U-shaped meandered slot microstrip patch antenna was proposed that works for biomedical applications [25]. Several researchers have proposed different bio-inspired optimization approaches such as Artificial Neural Network (ANN), Bacterial Foraging Optimization (BFO), Particle Swarm Optimization (PSO), etc for the fractal and hybrid fractal antenna designs. The utilization of ANN for the construction of hybrid fractal antenna that covers two distinct biomedical bands is explained in [26]. The estimation of various performance parameters related to circular patch antennas by means of neurocomputational models is presented in [27]. Feiz et al. [28] have explained the geometry of a microstrip antenna in which PSO technique was applied for the optimization of metamaterial structure. Two different optimization techniques such as FA and PSO were utilized for the synthesis of linear antenna array [29]. Mohammed et al. [30] have illustrated the use of PSO and FA algorithms for the design of a compact planer monopole antenna that works for UWB applications. A performance comparison of the Sierpinski gasket fractal antenna by employing different optimization techniques is done in [31]. The procedure for designing flower shaped microstrip patch antenna using ANN and FA algorithms is discussed in [32]. The use of two different algorithms such as PSO and FA on ten nonlinear benchmark functions is explained in [33]. Kaur and Sivia [34] have illustrated hybrid fractal antenna geometry for biomedical applications by optimizing its feed position through ANN and PSO.

The manuscript is organized in the following manner: — Section 2 describes the design procedure of proposed antenna along with all its geometrical details. ANN-based analysis model for the proposed GCSA is demonstrated in Section 3, and the procedure of curve fitting technique is illustrated in Section 4. Section 5 explains the use of FA for the feed position optimization. The simulated, optimized, and experimental results are described in Section 6. In the end, the conclusion is presented in Section 7.

2. PROPOSED HYBRID FRACTAL ANTENNA DESIGN

The proposed GCSA structure is a unique compounded fractal design which is formed by the composition of Giuseppe Peano, Cantor set and Sierpinski carpet fractals. In this design, the microstrip line feed position is optimized by using firefly algorithm. The integration of three different fractals helps to design a novel fractal geometry that exhibits special characteristics. A commercially available 1.6 mm thick, FR4 substrate with a dielectric constant of 4.4 is used in the proposed GCSA design. The patch dimensions are computed by using basic transmission line Equations (1)–(2) [34, 35]. A $50\ \Omega$ microstrip line feed with length ' L_f ' and ' W_f ' is placed at the optimized position along the y -axis and is connected with the designed patch. The feed position greatly affects the antenna performance characteristics. The proposed antenna represents a compact structure of size $34 \times 34\ \text{mm}^2$. The dimensions of the ground plane are $13.3 \times 34\ \text{mm}^2$. A rectangular slot is removed from the ground structure that results in an excellent gain. Figure 1 illustrates the structure of the proposed GCSA. Table 1 illustrates the geometrical specifications of proposed GCSA.

Table 1. Geometrical specifications of proposed GCSA.

S. No.	Design Parameter	Description	Value (mm)
1	L_s	Length of the used substrate	34
2	W_s	Width of the used substrate	34
3	L_p	Length of radiator	29
4	W_p	Width of radiator	29
5	L_f	Length of microstrip line feed	2.5
6	W_f	Width of microstrip line feed	3
7	L_g	Length of ground structure	13.3
8	W_g	Width of ground structure	34

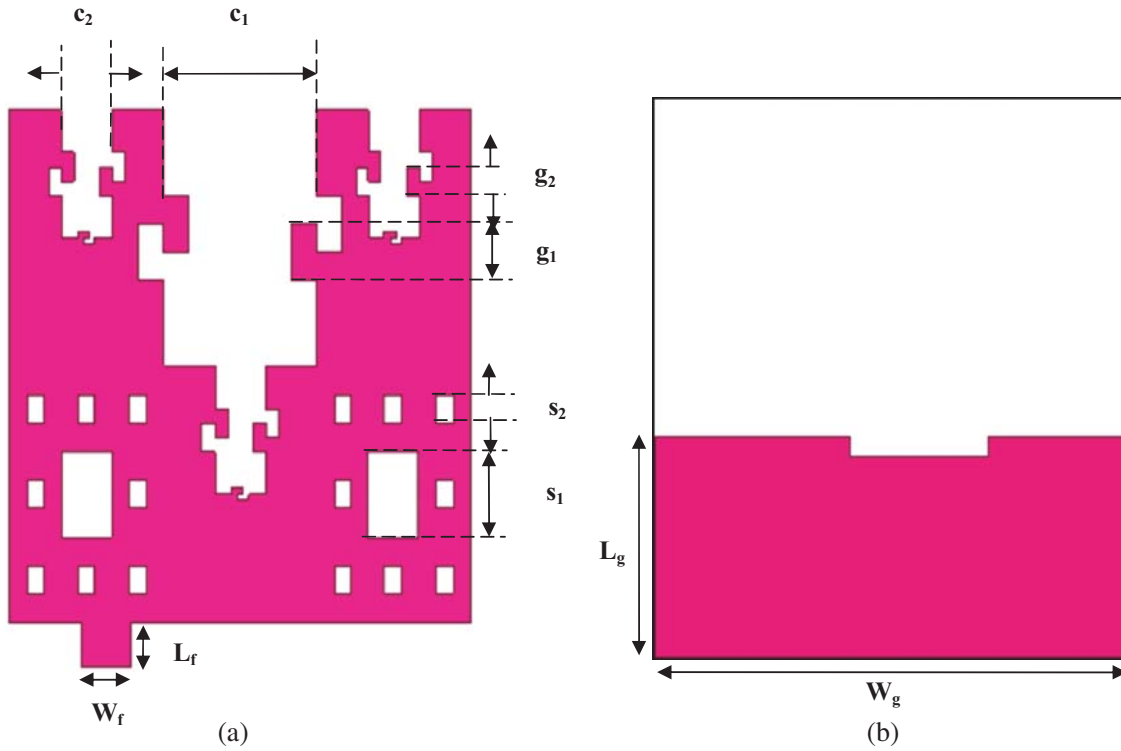


Figure 1. (a) Proposed GCSA design. (b) Ground plane.

The mathematical formula used to compute the resonance frequency f_r is given below [34]:

$$f_r = \frac{c}{2L_{eff}\sqrt{\epsilon_{eff}}} \quad (1)$$

The width W_p of the patch antenna is obtained by employing an equation given below [34]:

$$W_p = \frac{v_o}{2f_r} \sqrt{\frac{2}{\epsilon_r + 1}} \quad (2)$$

where ϵ_r = dielectric constant of used substrate, W_p = basic patch width, and ϵ_{reff} = effective dielectric constant.

3. ANN CONFIGURATION

In several disciplines, Artificial Neural Networks (ANNs) have been selected as powerful tools for modeling and prediction. ANNs are very beneficial for the antenna design and analysis [20]. Generally, the ANN architecture is obtained by the interconnection of three main layers. The layer which receives an input is termed as input layer. The output layer produces an overall output of the network [38]. The layer which is created between the input and output layers is referred as hidden layer. In successive layers, each neuron is linked to other neurons through direct communication links, and each communication link is associated with a weight value. The information about an input signal is present in the weights [38]. The network uses this information to solve various engineering problems. The error signal is generated by subtracting the network output from the desired output. Therefore, an ANN has the same capability just as the human brain [38]. Figure 2 describes an ANN-based analysis model for proposed GCSA. The proposed FFBN-ANN model configuration is specified in Table 2.

The expression used to formulate an absolute error is given below [34]:

$$\text{Absolute error} = [\text{Desired output} - \text{ANN model output}] \quad (3)$$

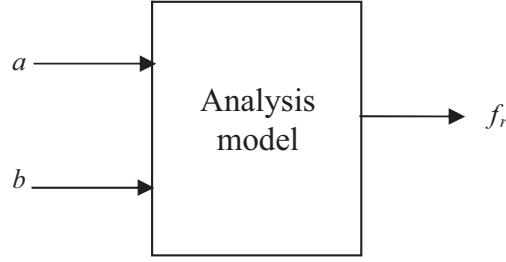


Figure 2. ANN-based analysis model for proposed GCSA.

Table 2. Simulated performance parameters of first and second iterations.

Iteration no.	Operating frequency (GHz)	S(1,1) (dB)	Gain (dB)
First	2.4411	-13.62	8.39
	5.7389	-11.40	7.17
Second	2.4341	-56.02	14.84

4. CURVE FITTING IMPLEMENTATION

Curve fitting is a statistical approach for generating mathematical relationships between various dependent and independent parameters in the form of a curve or a mathematical equation according to a given data set [34]. In other words, it deals with the evaluation of an appropriate model which is used to represent mathematical connection among the variables. Hence, this technique specifies a model that allows the best fit according to the provided data set [34]. A total of 58 samples is generated by varying the feed position of the proposed GCSA along the y -axis. By applying these values, the following mathematical equation is developed that indicates an association between the microstrip line feed position (y) and the resonant frequency (f_r).

$$f_r = 2.461 \sin(0.1259y + 6.949) + 0.0306 \sin(1.124y + 9.128) + 0.002287 \sin(7.366y - 13.29) \\ + 0.002519 \sin(8.732y - 7.318) + 0.001725 \sin(11.08y - 0.5975) - 0.0009745 \sin(14.5y - 9.16) \quad (4)$$

5. FA REALIZATION

Firefly algorithm is an effective, nature-inspired optimization technique which is influenced by the flashing properties of fireflies [32]. The flashing nature of fireflies helps them to locate their mates, attract possible preys and provide protection from predators. Bioluminescence is a process that allows the fireflies to create varying flashing patterns.

The firefly algorithm is dependent on the three basic rules that are given below [33]: —

- All fireflies are easily attracted towards each other regardless of their gender.
- Attractiveness is directly linked with flashing brightness. Each firefly is attracted by the flashing brightness of other fireflies, and therefore less attractive firefly tends to shift towards more attractive firefly.
- The firefly's brightness corresponds to the objective function.

In this algorithm, the changes in intensity of light and attractiveness formulation are the two significant issues. The attractiveness is mainly associated with an important parameter called as light intensity. The variation in light intensity with distance can be represented in two ways: by following the principle of inverse square law and due to the phenomenon of absorption that occurs in the transmission media. Thus, the formula for light intensity $L(d)$ is given by [32]:

$$L(d) = L_o e^{-\gamma d^2} \quad (5)$$

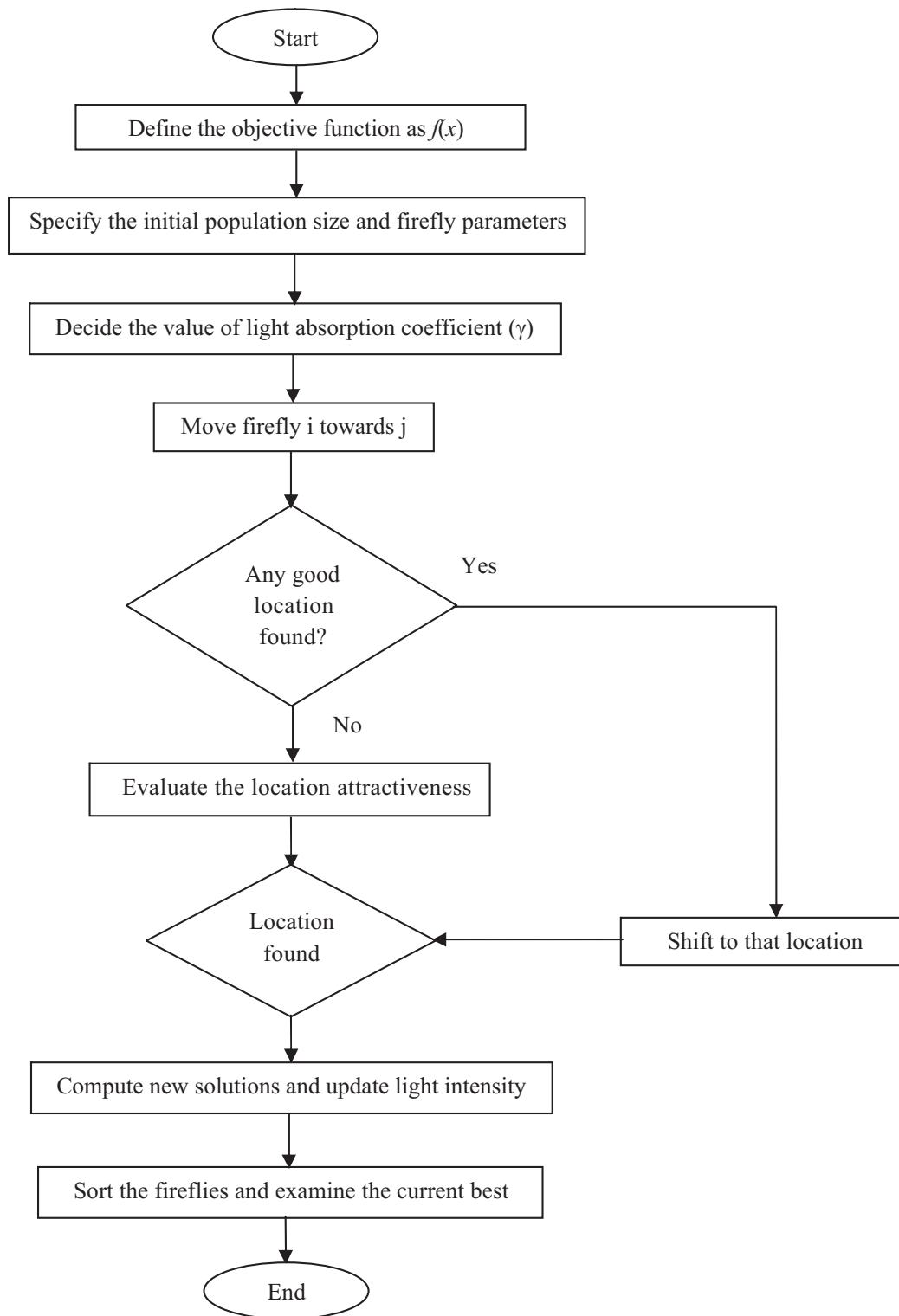


Figure 3. Flowchart of FA.

where L_o = light intensity in the beginning and γ = absorption coefficient related to light.

The attractiveness is concerned with light intensity observed by the fireflies, which are close to each other [30]. The expression used to define the attractiveness is given below [30]:

$$\beta = \beta_o e^{-\gamma d^2} \quad (6)$$

where β_o = predefined attractiveness.

The separation between i th firefly and j th firefly at x_i and x_j can be formulated as [32]:

$$d_{ij} = \|x_i - x_j\| \quad (7)$$

For updating the positions of fireflies, the changes are evaluated by [30]:

$$x_i^{m+1} = x_i^m + \beta_o e^{-\gamma d_{ij}^2} (x_j - x_i^m) + \alpha \left(rand - \frac{1}{2} \right) \quad (8)$$

Here, the second term in Eq. (8) represents the effect of attraction, and third term specifies the randomization, which consists of randomization parameter α and an arbitrary random number $rand$.

The developed cost function for this particular problem is presented in Eq. (9). This equation is used to evaluate the optimal value of feed position so that the proposed GCSA can operate at the desired frequency band. After some predefined number of iterations, the FA provides the best cost and optimal feed position value. Figure 3 represents the flowchart of FA.

$$\text{Cost function} = \sqrt[3]{(2.4341 - f_r)^2} \quad (9)$$

6. RESULTS AND DISCUSSIONS

6.1. Proposed GCSA Results

In order to investigate the performance of proposed GCSA, the swept frequency range from 2 to 9 GHz is selected. For the first iteration structure, the two frequency bands from 2.3518–2.5094 GHz and 5.6654–5.8002 GHz are examined with center frequencies of 2.4411 and 5.7389 GHz, respectively. The $S(1,1)$ values -13.62 and -11.40 dB are evaluated at the corresponding resonant frequencies. Figure 4 illustrates the simulated $S(1,1)$ characteristics for the first and second iterations. Figure 4 shows that there is shifting of frequency towards the lower side which indicates miniaturization of the desired structure. Simulated performance parameters of first and second iterations are depicted in Table 2. From the results, it is evaluated that the proposed GCSA contributes to miniaturization and is useful for biomedical applications.

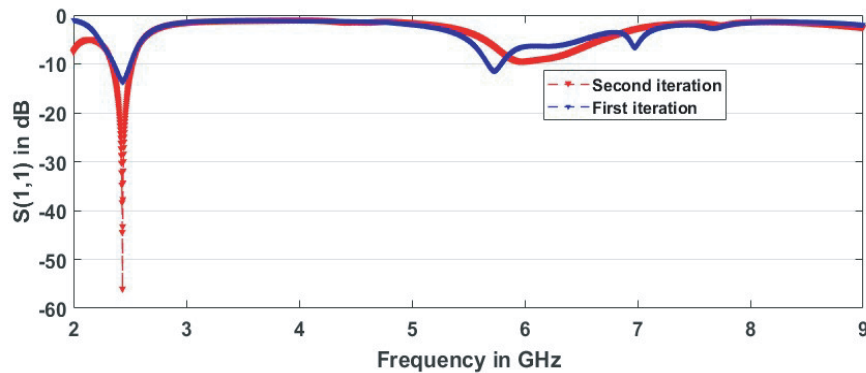


Figure 4. $S(1,1)$ characteristics of first and second iteration designs.

Figure 5 shows the pictorial view of fabricated GCSA. The fabricated prototype is experimentally verified by employing Vector Network Analyzer so as to assess its performance. Figure 6 illustrates the simulated and experimental $S(1,1)$ characteristics of proposed GCSA. It is found that the measured

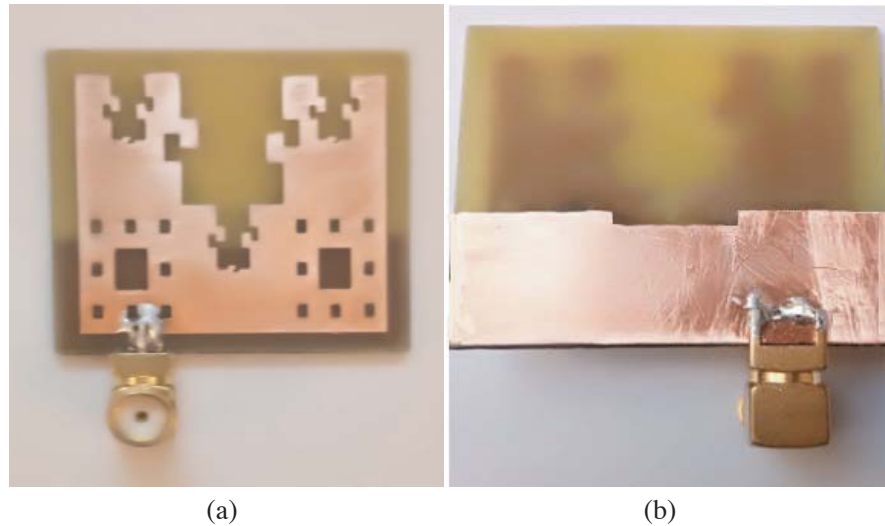


Figure 5. Fabricated GCSA prototype. (a) Front view. (b) Back view.

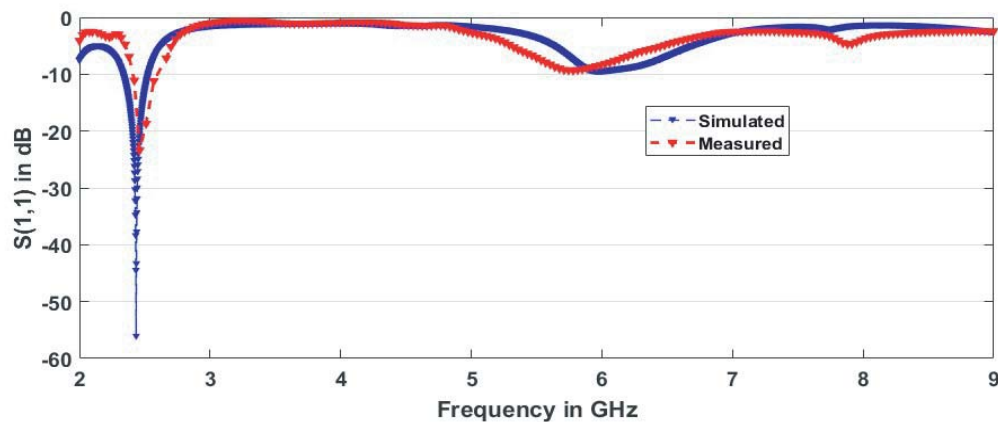


Figure 6. Simulated and experimental $S(1,1)$ characteristics of proposed GCSA.

resonance frequency is 2.4450 GHz with $S(1,1)$ value -23.4 dB. The measured bandwidth within the ISM band is 101 MHz. Both simulation and experimental results are shown to validate the design. It is found that experimental results show good match with the simulation ones. The proposed GCSA covers an important 2.45 GHz ISM band.

The surface current distribution on the surface of an antenna specifies its performance and radiation characteristics in an effective way. The simulated current distribution on the proposed GCSA at 2.4341 GHz is illustrated in Figure 7. It is observed that current predominantly flows at the feed and at the lower part of the designed patch. This part is responsible for good $S(1,1)$ value. Figure 8 demonstrates that a gain of 14.84 dB is achieved at an operating frequency of 2.4341 GHz. Figure 9 represents the plot of simulated and measured gains for proposed GCSA. The significant parameter to evaluate the distribution of radiation energy is the radiation pattern. The radiation pattern measurements are performed in an anechoic chamber. Figures 10(a), (b) show the comparison of simulated (dot line) and measured (dash line) far-field radiation patterns at 2.4341 GHz. It is evaluated that the radiation patterns are almost bidirectional, stable, and well matched.

Substrate material should be properly chosen so that it can satisfy the required electrical and mechanical specifications of the antenna [29]. The substrate materials used for investigation are: Taconic TLC-32 ($\epsilon_r = 3.2$), Rogers RO 4350 ($\epsilon_r = 3.66$), FR4 ($\epsilon_r = 4.4$), Arlon AD450 ($\epsilon_r = 4.5$) and Alumina ceramic ($\epsilon_r = 9.8$). The performance results by using these substrate materials are evaluated and

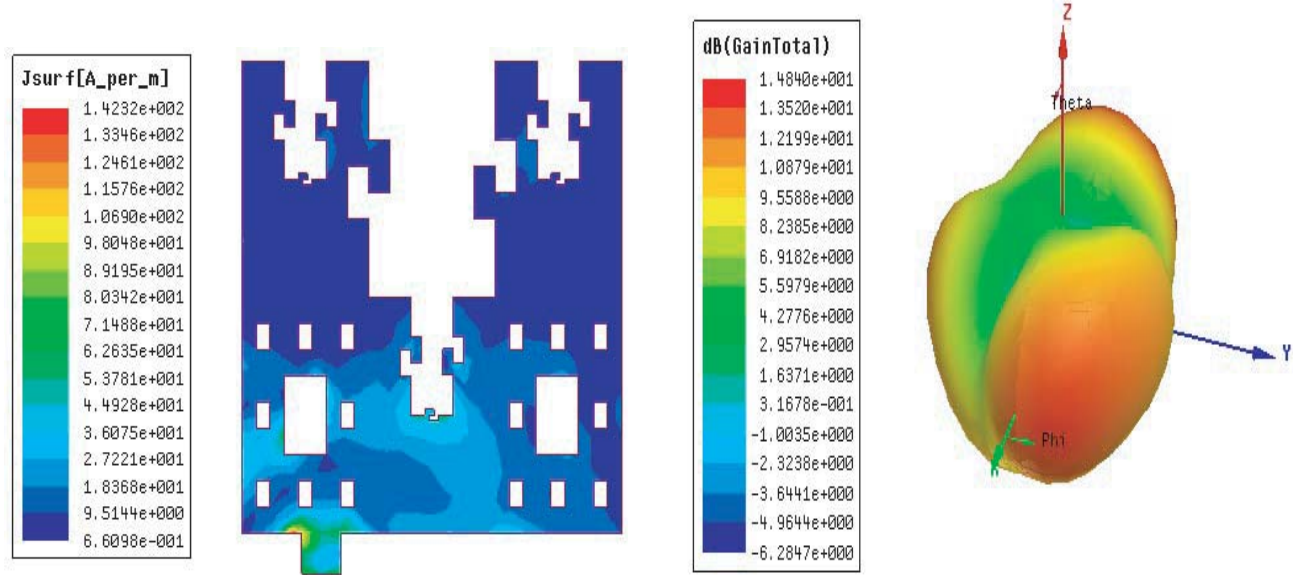


Figure 7. Surface current distribution at 2.4341 GHz.

Figure 8. Gain plot at 2.4341 GHz.

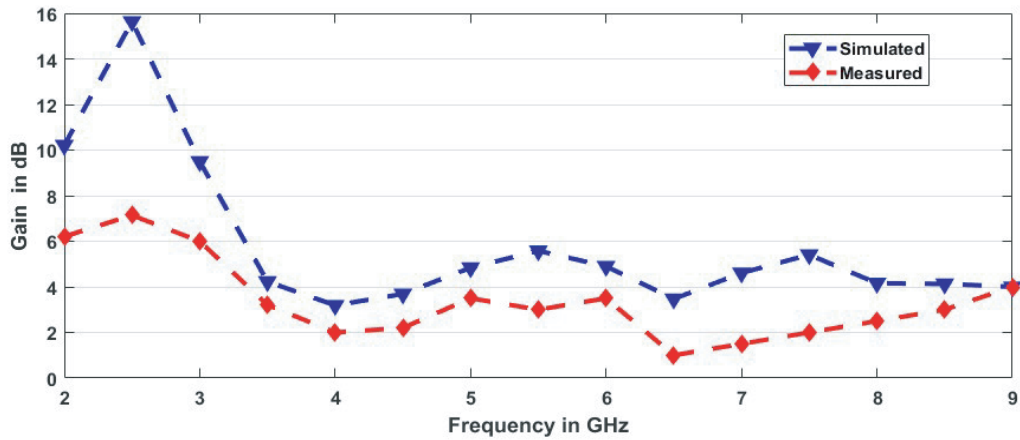


Figure 9. Simulated and measured gains of proposed GCSA.

Table 3. Performance results with five commonly employed substrates.

Substrate type	Dielectric constant	Dimensions of patch (mm ²)	Operating frequency (GHz)	S(1,1) (dB)	Gain (dB)
Taconic TLC-32	3.2	34 × 42	4.8095	-38.50	5.33
Rogers RO 4350	3.66	31 × 40	3.7137	-11.79	3.45
FR4	4.4	29 × 29	7.6889	-13.63	5.48
Arlon AD450	4.5	28 × 37	2.4341	-56.02	14.84
Alumina ceramic	9.8	19 × 26	6.4619	-10.49	8.30
			7.0413	-21.54	5.20
			8.6202	-13.39	7.60

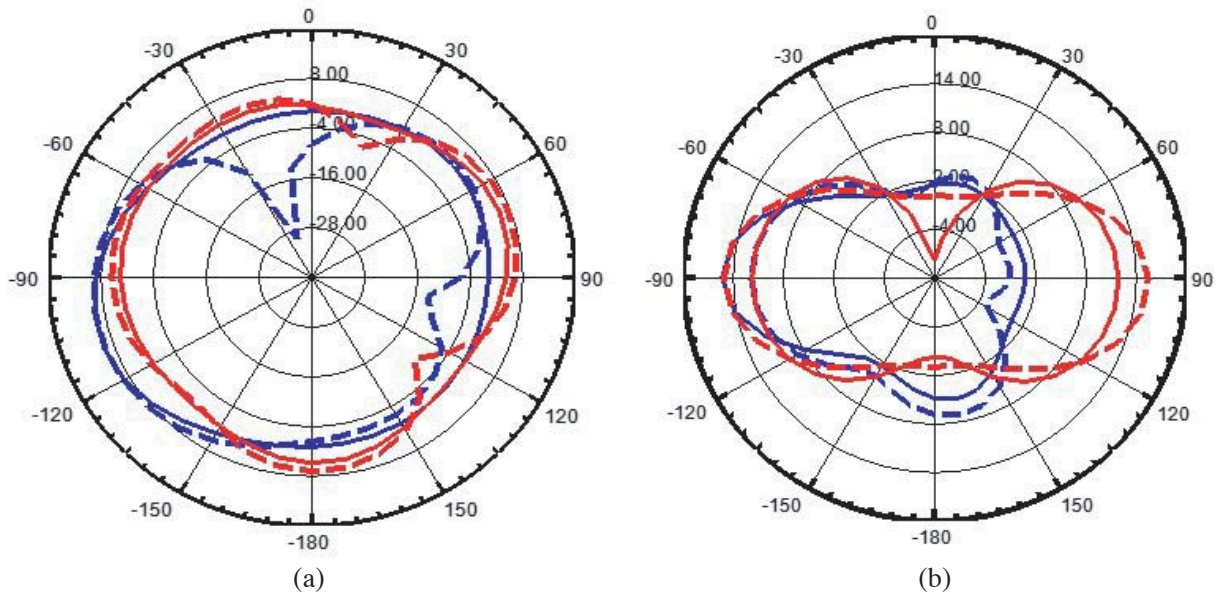


Figure 10. Simulated (solid line) and measured (dash line) far field radiation patterns in E and H planes (red line indicates co-polarization and blue line indicates cross-polarization) for proposed GCSA at (a) 2.4341 GHz (E Plane), (b) 2.4341 GHz (H Plane).

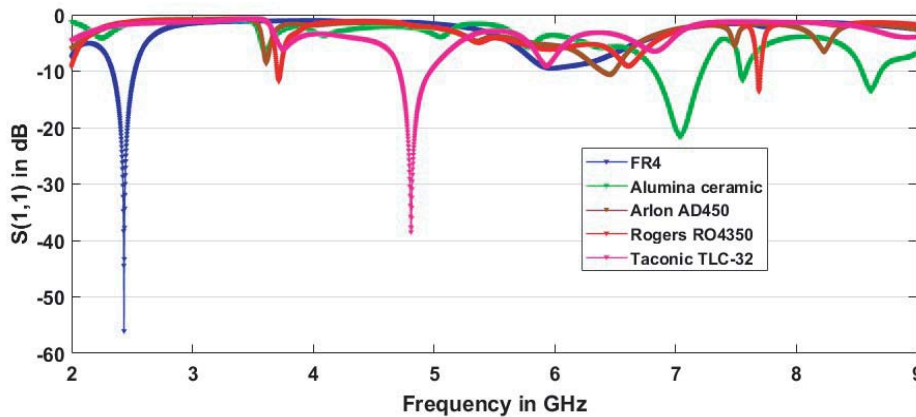


Figure 11. Simulated $S(1,1)$ characteristics of proposed GCSA with five different substrates.

compared in Table 3. Figure 11 represents the simulated $S(1,1)$ characteristics of proposed GCSA with five different substrates. From the comparison table, it is depicted that the relevant material is FR4 as it is economical and shows resonance at the desired frequency.

6.2. ANN Analysis of Proposed GCSA

The performance of three different ANN models using same set of 58 samples is evaluated in terms of average absolute error [36]. This parameter indicates the quality of training. A set of 58 GCSAs is created by varying length ‘ a ’ and width ‘ b ’ of the proposed structure. The estimated output is the resonant frequency. This designed set is used for the performance verification of three ANN models. A data set of 58 samples is divided into three subsets. Training subset consists of 40 samples. Each of the testing and validation subsets consists of 9 samples.

In FFBN type of ANN, there are two neurons at the input layer, ten neurons at the hidden layer, and one neuron at the output layer [36]. The employed training function is trainlm and the learning

Table 4. Comparison of all three ANN model outputs, related to f_r .

S. No.	Inputs		Resonant frequency f_r (GHz)				Absolute error		
	a	b	Desired output	FFBPN output	GRNN output	RBFNN output	FFBPN	GRNN	RBFNN
1	27	27	2.5619	2.5618	2.5151	2.4252	0.0001	0.0467	0.1366
2	27.5	28.5	2.4761	2.4609	2.4629	2.4772	0.0151	0.0131	-0.0011
3	28	28	2.4934	2.5006	2.4669	2.4623	-0.0071	0.0336	0.0382
4	28	28.5	2.4639	2.4599	2.4595	2.4734	0.0039	0.0043	-0.0095
5	28	29.5	2.4271	2.4238	2.4413	2.4424	0.0032	-0.0142	-0.0153
6	28.1	28.4	2.4659	2.4656	2.4603	2.4708	-0.0003	0.0052	-0.0052
7	28.1	28.7	2.4504	2.4564	2.4556	2.4699	-0.006	0.0012	-0.0131
8	28.2	30.6	2.3728	2.3699	2.4037	2.4194	0.0028	-0.0309	-0.0466
9	28.4	28.5	2.4589	2.4621	2.4564	2.4648	-0.0031	0.0056	-0.0027
10	28.7	27.8	2.4919	2.4862	2.4649	2.4441	0.0056	0.0269	0.0477
11	28.9	29	2.4289	2.4303	2.4416	2.4459	-0.0014	-0.0127	-0.0170
12	29	30	2.3798	2.3762	2.4105	2.4142	0.0035	-0.0307	-0.0345
13	29.1	28.1	2.4744	2.4751	2.4570	2.4481	-0.0007	0.0173	0.0262
14	29.9	28.1	2.4586	2.4711	2.4466	2.4447	-0.0125	0.0119	0.0138
15	29.9	28.9	2.4236	2.4174	2.4270	2.4096	0.0061	-0.0034	0.0139
16	30	28.9	2.4376	2.4145	2.4251	2.4059	0.0230	0.0124	0.0316
17	30	30.5	2.3571	2.3510	2.3725	2.3816	0.0060	-0.0154	-0.0245
18	30.5	29.7	2.3728	2.3580	2.3906	2.3433	0.0147	-0.0178	0.0294
19	30.8	28.7	2.4184	2.4091	2.4197	2.4234	0.0092	-0.0013	-0.0050
20	31	28	2.4516	2.4589	2.4352	2.4679	-0.0073	0.0163	-0.0163
Average absolute error							0.0027	0.0034	0.0073

rate parameter has value 0.15. In the case of Generalized Regression Neural Network (GRNN) type of ANN, the preferred value of spread constant is 0.9 and for Radial Basis Function Neural Network (RBFNN) type, this parameter has a value 1. The results of all ANN models are presented in Table 4. From this comparison table, it is observed that FFBPN has the smallest error value than GRNN and RBFNN. Hence, it is concluded that FFBPN is more accurate in estimating the resonant frequency for this particular problem. Figure 12 illustrates the graphical representation of FFBPN, GRNN, RBFNN and desired outputs, related to f_r and the average absolute errors of these ANNs are compared in Figure 13.

6.3. Firefly Algorithm Results

The firefly algorithm is implemented in MATLAB and applied so as to obtain the optimal value of the microstrip feed position. The parameter values selected for FA are as follows: number of iterations = 70; number of fireflies = 25; randomization parameter $\alpha = 0.25$; attractiveness at the initial value $\beta_o = 1$ and the value of light absorption coefficient $\gamma = 1$. By employing the cost function described in Eq. (9), the optimized feed position of proposed GCSA is 6.99. Figure 14 shows the graph of best cost against no. of iterations.

There are some important aspects to be considered while implementing an antenna for health care purposes [25]. The essential requirements are: small size, large gain, and easy to use. Table 5 reveals the comparison of proposed GCSA with some existing antennas. The designed structure has an initial area of 1156 mm², in contrast to other reported antennas. The proposed GCSA satisfy such requirements and performs better in terms of $S(1,1)$ characteristics, gain and bandwidth. Hence, this antenna is suggested as a suitable antenna for this kind of application.

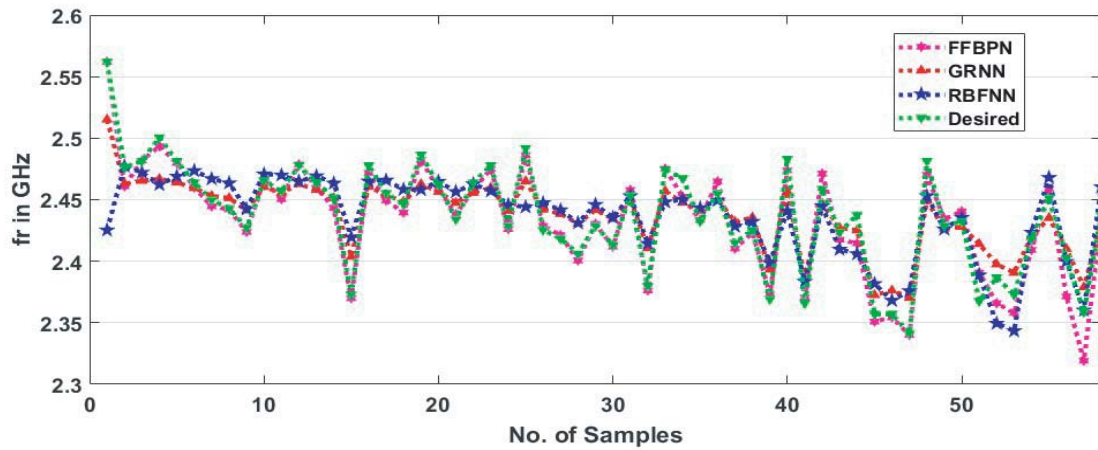


Figure 12. Comparison between FFBPN, GRNN and RBFNN and desired outputs, related to f_r .

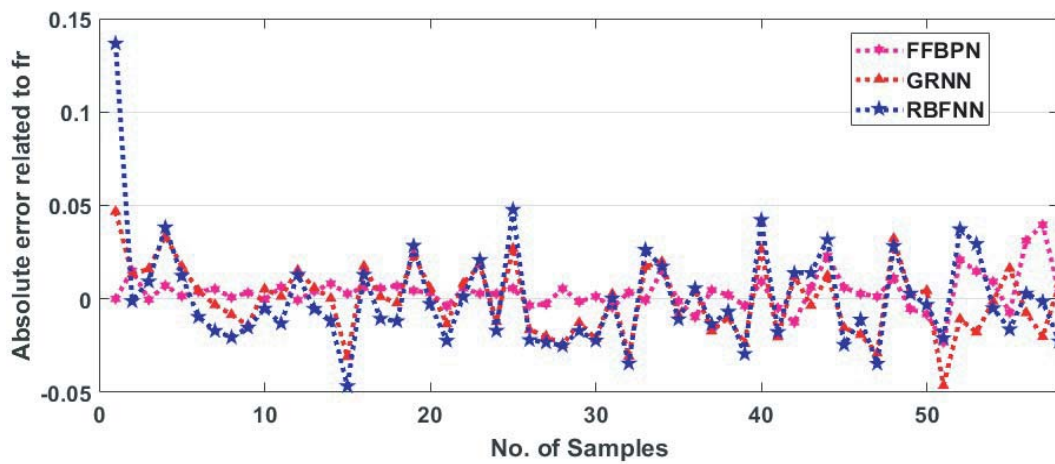


Figure 13. Comparison between absolute error of three ANN models, related to f_r .

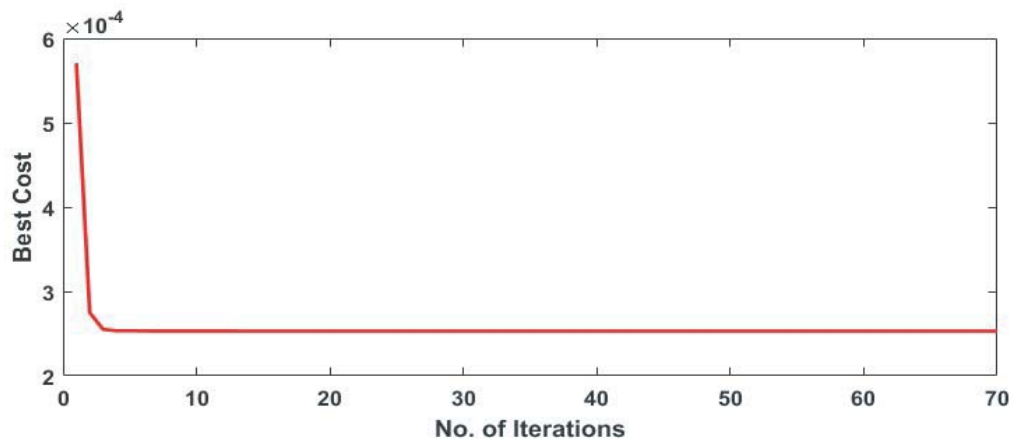


Figure 14. Best cost versus no. of iterations.

Table 5. Comparison of proposed GCSA with some existing antennas.

Reference No.	Area (mm ²)	S(1,1) dB	Substrate material used
[37]	800	-14.2	Jean
[21]	1610	-22	FR4 and Macor
[25]	1015	-43.72	FR4
Proposed GCSA	1156	-56.02	FR4

7. CONCLUSION

An approach for the feed position optimization of hybrid fractal antenna using firefly algorithm is presented in this paper. The proposed GCSA is designed by fusing Giuseppe Peano, Cantor set, and Sierpinski carpet fractals together. The designed antenna has a compact structure and resonates at 2.4411 GHz ISM band. The proposed GCSA exhibits a significant size reduction capability. The performance comparison of three different ANNs is done to find the best suitable type of ANN. The comparison of optimized results with simulated and measured results demonstrates that this approach is a possible option for experimental analysis.

ACKNOWLEDGMENT

The authors would like to thank National Institute of Technical Teachers Training and Research (NITTTR), Chandigarh and Indian Institute of Technology (IIT), New Delhi for providing the facility to test the fabricated prototype.

REFERENCES

1. Lin, W. and H. Wang, "Polarization reconfigurable circular patch antenna with multiple l-probes for biomedical applications," *IEEE International Symposium on Antennas and Propagation (APSURSI)*, Jul. 2016, ISSN: 1947-1491.
2. Hall, P. S. and Y. Hao, *Antennas and Propagation for Body-centric Communications*, Artech House, London and Boston, 2006.
3. Kaur, G., A. Kaur, G. K. Toor, B. S. Dhaliwal, and S. S. Pattnaik, "Antennas for biomedical applications," *Biomedical Engineering Letters*, Vol. 5, No. 3, 203–212, Sept. 2015.
4. Sabban, A., "New wideband printed antennas for medical applications," *IEEE Transactions on Antennas and Propagation*, Vol. 61, No. 1, 84–91, Jan. 2013.
5. Mandelbrot, B. B., *The Fractal Geometry of Nature*, W. H. Freeman, New York, 1983.
6. Ali, J. K., M. T. Yassen, M. R. Hussan, and A. J. Salim, "A printed fractal based slot antenna for multiband wireless communication applications," *Proceedings of PIERS*, 618–622, Moscow, Russia, Aug. 19–23, 2012.
7. Oraizi, H. and S. Hedayati, "Circularly polarized multiband microstrip antenna using square and giuseppe peano fractals," *IEEE Transactions on Antennas and Propagation*, Vol. 60, No. 7, 3466–3470, Jul. 2012.
8. Sundaram, A., M. Maddela, and R. Ramadoss, "Koch-Fractal folded-slot antenna characteristics," *IEEE Antennas and Wireless Propagation Letters*, Vol. 6, 219–222, Apr. 2007.
9. Oraizi, H. and S. Hedayati, "Combined fractal geometries for the design of wide band microstrip antennas with circular polarization," *PIERS Proceedings*, 1262–1267, Suzhou, China, Sept. 12–16, 2011.
10. Sharma, N., V. Sharma, and S. S. Bhatia, "A novel hybrid fractal antenna for wireless applications," *Progress In Electromagnetics Research M*, Vol. 73, 25–35, 2018.

11. Dhaliwal, B. S. and S. S. Pattnaik, "BFO-ANN ensemble hybrid algorithm to design compact fractal antenna for rectenna system," *International Journal on Neural Computing and Applications*, Vol. 28, No. 1, 917–928, Dec. 2017.
12. Singh, S. and B. S. Dhaliwal, "Analysis of hybrid fractal antenna using artificial neural network," *International Conference on Soft Computing in Wireless Communication (SCAWC 2017)*, 219–222, Mar. 9–11, 2017.
13. Kaur, K. and J. S. Sivia, "A compact hybrid multiband antenna for wireless applications," *International Journal on Wireless Personal Communications*, Vol. 97, No. 4, 5917–5927, Dec. 2017.
14. Sharma, N. and S. S. Bhatia, "Split ring resonator based multiband hybrid fractal antennas for wireless applications," *International Journal of Electronics and Communications*, Vol. 93, 39–52, Sept. 2018.
15. Bangi, I. K. and J. S. Sivia, "Minkowski and Hilbert curves based hybrid fractal antenna for wireless applications," *International Journal of Electronics and Communications*, Vol. 85, 159–168, Feb. 2018.
16. Brar, A. S., J. S. Sivia, and G. Bharti, "A compact hybrid Minkowski fractal antenna for C and X-band applications," *International Journal of Computer Science and Information Security (IJCSIS)*, Vol. 14, No. 12, 349–352, Dec. 2016.
17. Saputro, S. A. and J. Y. Chung, "Hilbert curve fractal antenna for dual on- and off-body communication," *Progress In Electromagnetics Research Letters*, Vol. 58, 81–88, 2016.
18. Choukiker, Y. K. and S. K. Behera, "Modified Sierpinski square fractal antenna covering ultra-wide band application with band notch characteristics," *IET Microwaves, Antennas & Propagation*, Vol. 8, No. 7, 506–512, May 2014.
19. Li, Y., X. Yang, C. Liu, and T. Jiang, "Miniaturization cantor set fractal ultrawideband antenna with a notch band characteristic," *Microwave and Optical Technology Letters*, Vol. 54, No. 5, 1227–1230, Mar. 2017.
20. Sivia, J. S., A. P. S. Pharwaha, and T. S. Kamal, "Analysis and design of circular fractal antenna using artificial neural networks," *Progress In Electromagnetics Research B*, Vol. 56, 251–267, 2013.
21. Salim, M. and A. Pourziad, "A novel reconfigurable spiral-shaped monopole antenna for biomedical applications," *Progress In Electromagnetics Research Letters*, Vol. 57, 79–84, 2015.
22. Oraizi, H. and S. Hedayati, "Miniaturized UWB monopole microstrip antenna design by the combination of Giuseppe Peano and Sierpinski Carpet fractals," *IEEE Antennas and Wireless Propagation Letters*, Vol. 10, 67–70, Jan. 2011.
23. Choukiker, Y. K. and S. K. Behera, "Design of wideband fractal antenna with combination of fractal geometries," *International Conference on Information, Communications and Signal Processing*, Singapore, Dec. 13–16, 2011.
24. Oraizi, H. and S. Hedayati, "Circularly polarized multiband microstrip antenna using square and Giuseppe Peano fractals," *IEEE Transactions on Antennas and Propagation*, Vol. 60, No. 7, 3466–3470, Jul. 2012.
25. Sukhija, S. and R. K. Sarin, "A U-shaped meandered slot antenna for biomedical applications," *Progress In Electromagnetics Research M*, Vol. 62, 65–77, 2017.
26. Kaur, M. and J. S. Sivia, "ANN-based design of hybrid fractal antenna for biomedical applications," *International Journal of Electronics*, Vol. 106, No. 8, 1184–1199, Mar. 2019.
27. Sivia, J. S., A. P. S. Pharwaha, and T. S. Kamal, "Neurocomputational models for parameter estimation of circular microstrip patch antennas," *Procedia Computer Science*, Vol. 85, 393–400, Dec. 2016.
28. Feiz, N., F. Mohajeri, and D. Zarifi, "Design, simulation and fabrication of an optimized microstrip antenna with metamaterial superstrate using particle swarm optimization," *Progress In Electromagnetics Research M*, Vol. 36, 101–108, May 2014.
29. Zaman, M. A. and M. A. Matin, "Nonuniformly spaced linear antenna array design using firefly algorithm," *International Journal of Microwave Science and Technology*, Vol. 2012, 1–8, Jan. 2012.

30. Mohammed, H. J., A. S. Abdullah, R. S. Ali, R. A. Abd-Alhameed, Y. I. Abdurraheem, and J. M. Noras, "Design of a unipolar printed triple band-rejected ultra-wideband antenna using particle swarm optimization and the firefly algorithm," *IET Microwaves, Antennas & Propagation*, Vol. 10, No. 1, 31–37, 2014.
31. Dhaliwal, B. S. and S. S. Pattnaik, "Performance comparison of bio-inspired optimization algorithms for Sierpinski gasket fractal antenna design," *Neural Computing and Applications*, Vol. 27, No. 3, 585–592, Apr. 2016.
32. Kaur, R. and M. Rattan, "Optimization of the return loss of differentially fed microstrip patch antenna using ANN and firefly algorithm," *Wireless Personal Communications*, Vol. 80, No. 4, 1547–1556, Feb. 2015.
33. Bhushan, B. and S. S. Pillai, "Particle swarm optimization and firefly algorithm: Performance analysis," *IEEE International Advances Computing Conference (IACC)*, 746–751, Feb. 22–23, 2013.
34. Kaur, M. and J. S. Sivia, "Minkowski, Giuseppe Peano and Koch curves based design of compact hybrid fractal antenna for biomedical applications using ANN and PSO," *International Journal of Electronics and Communications*, Vol. 99, 14–24, Feb. 2019.
35. Balanis, C. A., *Antenna Theory: Analysis and Design*, 3rd Edition, John Wiley & Sons, London.
36. Dhaliwal, B. S. and S. S. Pattnaik, "Artificial neural network analysis of Sierpinski Gasket fractal antenna: A low-cost alternative to experimentation," *Advances in Artificial Neural Systems*, Vol. 2013, Article ID 560969, 7 pages, Jan. 2013.
37. Gil, I. and R. Fernandez-Garcia, "Wearable PIFA antenna implemented on jean substrate for wireless body area network," *Journal of Electromagnetic Waves and Applications*, Vol. 31, No. 11–12, 1194–1204, 2017.
38. Sivanandam, S. N. and S. N. Deepa, *Principles of Soft Computing*, Wiley-India (P) Ltd., New Delhi, 2008.